Dielectric Spectroscopy of Human Erythrocytes: Investigations Under the Influence of Nystatin

J. Gimsa, Th. Schnelle, G. Zechel, and R. Glaser
Department of Biology, Humboldt-University, Invalidenstr. 42, D-10115 Berlin, Germany

ABSTRACT When placed in rotating electric fields red blood cells show a typical electrorotation spectrum with antifield rotation in the lower and cofield rotation in the higher frequency range. Assuming a spherical cell geometry, however, dielectrical parameters were obtained that differ from those measured by independent methods. Dielectrophoresis and, in particular, electrorotation yielded lower membrane capacitance values than expected. Introduction of an ellipsoidal model with an axis ratio of 1:2 allowed a description that proved to be consistent with dielectrophoresis and electrorotation data. For control cells an internal conductivity of 0.535 S/m, a specific membrane capacitance of 0.82×10^{-2} F/m^2, and a specific conductance of 480 S/m^2 were obtained. The first characteristic frequency (frequency of fastest antifield rotation) and the related rotation speed can be measured quite quickly by means of a compensation method. Thus it was possible to follow changes of dielectric properties on individual cells after nystatin application. Ionophore-membrane interaction caused cell shrinkage in parallel to a decrease of the first characteristic frequency and rotation speed. Analysis of data revealed a decrease of the internal conductivity that is not only caused by ion loss but also, to a large extent, by a strong increase of hindrance because of shrinkage. Ionophore-induced membrane permeabilities can be calculated from volume decrease as well as from electrorotational data. In no case can these permeabilities count for the high membrane-AC conductivity that is attributed to the band-3 anion exchanging protein. The membrane-AC conductance was found not to be decreased for cells in Donnan equilibrium, which had leaked out almost completely.

INTRODUCTION

In contrast to usual impedance measurements on cell suspensions, dielectrophoresis and electrorotation both offer a unique capability of monitoring the dielectric properties of single cells. It was shown that these methods are suitable for determining specific membrane capacitance, membrane conductance, and cytoplasmic conductivity (Asami et al., 1989; Burt et al., 1990; Donath et al., 1990; Engel et al., 1988; Fuhr et al., 1985, 1986; Gascoyne et al., 1993; Georgiewa et al., 1989*b*; Gimsa et al., 1988, 1989, 1991; Huang et al., 1992; Kaler and Jones, 1990; Kaler et al., 1992; Marszalek et al., 1991; Miller and Jones, 1993; Müller et al., 1993; Pastushenko et al., 1985; Wang et al., 1992). For such measurements, however, only a few cells immersed in a very low ionic strength suspension medium (< 5 mM salt) are required. When exposed to a nonuniform electrical field ($\vec{E}$), the cells experience a dielectrophoretic force ($\vec{F}$). This force can be calculated from the field gradient and the polarization vector ($\vec{P}$)

$$\vec{F} = (\vec{P}\nabla)\vec{E}. \quad (1)$$

For sufficiently high field frequencies, the induced charges follow the field with a delay. In the case of rotating fields, this produces a torque (N) that depends on field frequency and relaxation time of the induced polarization

$$\vec{N} = \vec{P} \times \vec{E}. \quad (2)$$

For simple geometries of the cell model, like multishelled spheres (Fuhr et al., 1985; Huang et al., 1992; Irimajiri et al., 1991) and confocal, multishelled ellipsoids (Asami et al., 1980; Müller et al., 1993; Paul and Otwinowski, 1991; Stepin, 1965), the polarization can be expressed analytically as a function of the dielectric parameters of the assumed model. With one single shell these two models were applied to erythrocytes (for spherical model see Burt et al., 1990; Gascoyne et al., 1993; Gimsa et al., 1988, 1989; for ellipsoidal model see Kinosita and Tsong, 1977; Miller and Jones, 1993; Stenger et al., 1991). In this study, we applied the more realistic ellipsoidal single-shell model. This decision was made because independent methods yielded different dielectric parameter values for the spherical single-shell model.

To determine the cellular dielectric parameters, two general methods can be invoked: whole frequency spectra can be fitted to a model, or, alternatively, the dependence of characteristic spectra points on an independent parameter (like medium conductivity) can be measured. We measured the dependence of two characteristic points, the first critical frequency of dielectrophoresis and the first characteristic frequency of electrorotation, on the external medium conductivity. These two frequencies are related to the dispersion of membrane polarization. Thus, they are strongly determined by membrane and internal cellular properties.

Erythrocytes suspended in external media of low ionic strength undergo certain changes such as shrinkage and ion loss (Georgiewa et al., 1989a, b; Glaser, 1982, 1984). Under the influence of ionophores, these processes are enhanced

Received for publication 23 August 1993 and in final form 14 January 1994.
Address reprint requests to Jan Gimsa, Department of Biology, Humboldt-Universität zu Berlin, Invalidenstr. 42, D-10115 Berlin, Germany. Tel.: 49-30-2897-2692; fax: 49-30-2897-2520; E-mail: jan=gimsa@rz.hu-berlin.de.

0006-3495/94/04/1244/10 $2.00

even further. Such physical and physicochemical changes are reflected in their dielectric properties because of changes of cell geometry, membrane properties, and internal conductivity. This study deals with the temporal changes in the cell dielectric properties after suspension in low ionic strength media under the influence of nystatin. For fast detection of changes in the dielectric properties, we used a special feature of the electrorotational spectrum: that the dielectric dispersion of membrane polarization, which is directly related to the antifield rotation, is a peak (see Fig. 3). This allows the application of a compensation method (Arnold and Zimmerman, 1983; Gimsa et al., 1989, 1991) to follow changes in the frequency of the antifield rotation peak of individual erythrocytes.

MATERIALS AND METHODS

Erythrocytes

For measurements human citrate blood from healthy donors was supplied by the blood bank of Charité Humboldt University, Berlin. It was stored no longer than 5 days in an ACD stabilizer-medium at 4°C. For all experiments the plasma and buffy coat were removed after centrifugation at 500 × *g* for 10 min followed by two washes in Krebs-Ringer solution, pH 7.4, for 10 min at 2000 × *g*. Red cells were resuspended in Krebs-Ringer solution at a hematocrit of 10%. For volume, dielectrophoresis, and electrorotation experiments, however, a hematocrit of 0.02% was used.

Measuring solution for electrorotation

A 300-mOsm solution of sucrose containing 1-mM phosphate buffer (pH 6.8) was used. The conductivity of the measuring solution containing cells at a hematocrit of 0.02% was about 12.5 mS/m.

Ionophore solutions

Nystatin (Calbiochem, Bad Soden, Germany, and Behring Corp., Marburg Lahn, Germany) was diluted at a concentration of 5 mM in dimethylformamide (DMF). This stock solution was stored at −18°C. For measurements various amounts of stock solution were added to the measuring solution before suspending the cells.

Measurement of internal conductivity

To obtain internal conductivity values independently from electrorotation measurements, different experiments corresponding to different cell states were carried out. In all cases, after washing in Krebs-Ringer solution cells were washed once in the measuring solution. Then erythrocytes were adapted to the desired cell ionic state in the measuring solution and under the influence of the ionophore. To allow cell handling in all cases a hematocrit of 2.5% was used for incubation. Cells were spun down and subsequently diluted to hematocrits of approximately 20, 40, 60, and 80%. By addition of Triton × 100 they were hemolyzed, and the conductivity was measured with a conductometer (Schott, Hofheim, Germany CG855).

Cell volume measurements

Relative cell volumes were measured with a Coulter-counter (model Laborscale PSL1, Medicor, Budapest, Hungary). Because erythrocytes are not spherical in shape and because their shape changes with volume, a calibration curve was measured in the following way: a 08 mM NaCl solution with 5.8-mM phosphate buffer (pH 6.8) was supplemented by sucrose and distilled water to achieve different osmotic pressure solutions over the range 250–625 mOsm. Erythrocytes suspended in these solutions were fixed by 0.1% glutaraldehyde after volume adaptation (15 min). Their size distribution was measured by a Coulter-counter. The measured channel-number distribution function was statistically interpreted, and the mean channel number was assumed to represent a certain erythrocyte volume that corresponds to the relative red cell volume in the C-state determined from the ionic-state model of Glaser et al. (1984). With this channel-number volume relation established, the time dependence of cell volume under the influence of ionophores was checked. Parallel with the time course of electrorotation measurements, cells from the suspension were fixed. For volume determination of these cells a NaCl solution was added to increase the external conductivity to the value used to determine the calibration curve.

External electric field in electrorotation

Experiments were conducted in a four-electrode chamber with electrode distances of 1.5 mm. The electrodes were driven by four 90° phase-shifted symmetrical square wave signals of 10 V_{PP} amplitude. The induced cell rotation speed was on the order of one revolution per second, sufficiently high for measurements with the compensation method. Electrorotation spectra for symmetrical square wave fields have been shown to be only slightly disturbed by the higher harmonics (Gimsa et al., 1988). Therefore, sinusoidal fields were used for calculations of the dielectric response of the cells.

Electrorotation measurements

The rotation of cells subjected to a rotating electric field was investigated microscopically. Measurements were performed on cells in suspension using an inverted optical microscope. For measurements cells were suspended at a concentration of 0.02% before transfer to the measuring chamber. For ionophore treatment, a desired concentration of ionophore was added to the measuring solution before the cell suspension. The first characteristic frequency (see f_{c1} in Fig. 3) of the cells under investigation was followed by a compensation method (Arnold and Zimmermann, 1983). For compensation two frequencies having a constant frequency ratio of 4 but different senses of rotation were alternately applied. When cell rotation ceased the characteristic frequency was the geometrical average of the two frequencies. At this frequency the rotation speed (see R_{min} in Fig. 3) was determined by switching the compensation field to the normally rotating field. The first characteristic frequency of one and the same cell was followed for several min. All measurements were carried out at a room temperature of about 23°C.

Measurement of dielectrophoresis and electrorotation of control cells

To determine the electrical parameters of control cells, the first characteristic frequency of electrorotation and first critical frequency of dielectrophoresis were measured within 4 min after suspension of cells into solutions of different conductivities. The solution conductivity was adjusted by the addition of NaCl. To obtain conductivity values lower than 0.01 S/m, no phosphate buffer was added. For electrorotation, the first characteristic frequency but not the rotation speed was determined. Dielectrophoretic measurements were carried out in a separate measuring chamber consisting of a platinum needle opposing a platinum plate electrode at a distance of about 300 μm. Only the first critical frequency of the dielectrophoretic spectrum was determined (Gimsa et al., 1991; Kaler and Jones, 1990; Kaler et al., 1992; Marszalek et al., 1991). Because at this frequency cell movement ceases, it was not necessary to determine dielectrophoretic mobilities, which is a complex problem within an area of changing field gradient. For the above measurements a sine-wave generator with a peak-to-peak output voltage of 3 V was adjusted to a frequency at which cell movement ceased.

EXPERIMENTAL RESULTS

Measurement of the internal conductivity

To determine the internal conductivity, the procedure of Fricke (1953) was adopted, as described under Materials and Methods. Three different experiments corresponding to three different cell states were carried out. The first experiment was designed to measure the internal conductivity immediately after the cells were introduced into the measuring solution; after washing, the conductivities of hemolysates at different hematocrits were measured. In the second experiment, cells were incubated in the measuring solution for 30 min at room temperature. They were spun down and diluted before hemolysis. The third experiment was designed to measure the internal conductivity in Donnan-osmotic equilibrium, after complete leakage of the cytoplasmatic ions. In this case nystatin was added during incubation at a concentration of 20 μg/ml. To insure that the external ion concentration did not significantly increase from the leaked ions, the cells were spun down after 30 min and incubated once again. After this treatment cells were more adhesive, which caused problems for the adjustment of hematocrits larger than 60%.

Every point in Fig. 1 (Table 1) represents four measurements. The curves are nonlinear regression-fits of the phenomenological function (Georgiewa et al., 1989*b*)

$$\sigma = \sigma_0 + \sigma_e(1 - \exp(-\lambda H_K)). \quad (3)$$

The coefficients σ, σ_0 and H_K represent the conductivity at a certain hematocrit, conductivity of the measuring solution, and the hematocrit. σ_e and λ were fitted to measured points. Cytoplasmatic conductivity values (σ_i) were obtained from Eq. 3 at a hematocrit of 100%.

Cell volume dependence on ionophore concentration

The volume dependence of erythrocytes was measured to obtain information about the ionophore-induced membrane permeability increase. The time dependence of erythrocyte volumes was investigated under the influence of different nystatin concentrations. Volume distributions were measured as described under Materials and Methods. For simplicity error bars in Fig. 2 were not plotted. For all points the average error was about ±6% of their absolute value.

After transfer into the measuring solution at any ionophore concentration cells shrunk to a volume of 88.3% within less than half a min. The shrinkage continued at a rate that depended on the ionophore concentration. At a concentration of 40 μg/ml nystatin, a minimum of 51% was reached after 6 min. Curves in Fig. 2 indicate that for higher ionophore concentrations a minimum is reached only transiently, followed by an apparent swelling. At higher concentrations the volume could not be followed for 30 min. To understand the volume increase the time dependence of cell shape must be taken into account. Erythrocytes undergo volume changes with the membrane surface area remaining constant. Thus any volume change is accompanied by a shape change. Microscopic observations showed that the dominating biconcave shape during the first minutes of suspension changes to a stomatocytic shape. This shape transformation rate increases with increasing ionophore concentration. Finally stomatocytes tend to become spherical, entrapping a certain volume of external solution. The entrapped volume becomes

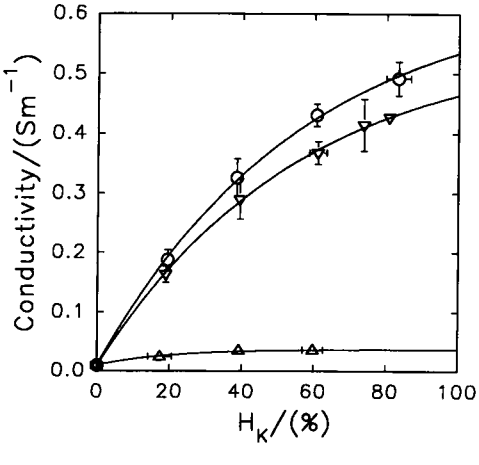

FIGURE 1 Conductivity of erythrocyte suspensions after hemolysis at different hematocrits: without incubation in measuring solution (control, ○), after suspension for 30 min (▽), and after nystatin treatment (△).

TABLE 1 Conductivity of erythrocyte suspensions after hemolysis at different hematocrits

	σ_0 (mS/m)	λ (l/%)	σ_i (mS/m)
After suspension (control)	9.3	0.0177	535
After 30 min of incubation	8.8	0.0182	464
Donnan-equilibrium	9.9	0.0509	37

Coefficients were obtained by fitting Eq. 1, with σ_i standing for the extrapolated cytoplasmic conductivity.

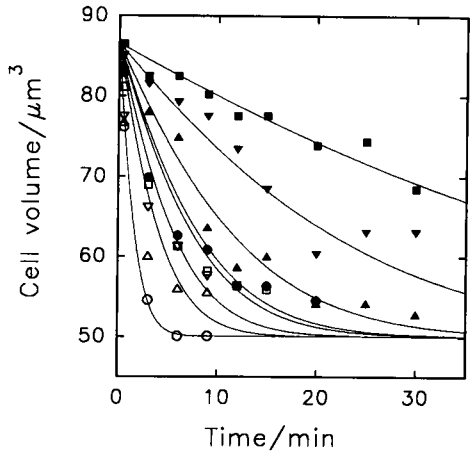

FIGURE 2 Volume dependence of ionophore-treated erythrocytes on time. Curves are fit according to Eq. A4. For the different concentrations (in μg/ml) the following permeabilities, P (in m/s), were calculated: 0 (■, $P = 2.1 \times 10^{-10}$), 10 (▼, $P = 4.4 \times 10^{-10}$), 15 (▲, $P = 8.3 \times 10^{-10}$), 20 (●, $P = 1.2 \times 10^{-9}$), 25 (□, $P = 1.3 \times 10^{-9}$), 30 (▽, $P = 1.7 \times 10^{-9}$), 35 (△, $P = 2.3 \times 10^{-9}$), and 40 μg/ml (○, $P = 5.8 \times 10^{-9}$).

inaccessible to DC electric current. This may possibly be the reason for the apparent increase in volume at higher ionophore concentrations. For varied ionophore concentrations not all curves attain a minimum of about 51% of the native cell volume. This is the result of a different shape at a given cell volume. Microscopically for control cells within the first 5 min after suspension, a diameter of 6.6 ± 0.5 μm was found.

Measurement of dielectric parameters of control cells

On control cells immediately after suspension in measuring solution, complete electrorotation spectra were measured over the accessable frequency range. Data of 10 cells are presented in Fig. 3:

The first critical frequency of dielectrophoresis and the first characteristic frequency of electrorotation of control cells in dependence on the external medium conductivity were determined within 5 min after suspending the cells into measuring solution (Fig. 4, *A* and *B*).

Influence of DMF

To check whether the measured effects of ionophore action on the first characteristic frequency were partially caused by DMF, results of control cells were compared with cells measured under the influence of the maximum amount of DMF (applied when the highest ionophore concentrations were used). No difference could be found.

Ionophore action on the first characteristic frequency (f_{c1}) and the antifield rotation peak (R_{min})

The first characteristic frequency changes were followed repetitively for 30 min, starting about 2 min after suspension.

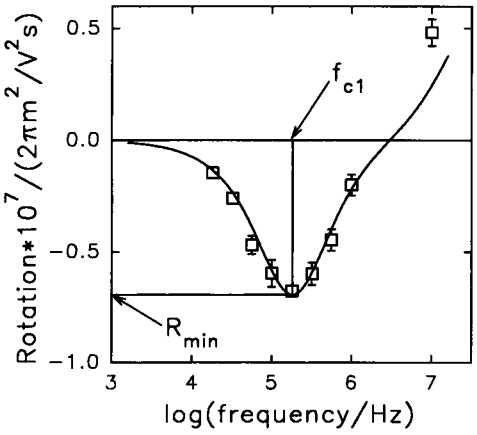

FIGURE 3 Electrorotational spectrum of erythrocytes in the frequency range of 10 kHz to 10 MHz at 12.5 mS/m external conductivity. Data were fitted to a phenomenological curve according to a single-shell model. For the antifield rotation the first characteristic frequency (f_{c1}) and the rotation peak (R_{min}) are depicted.

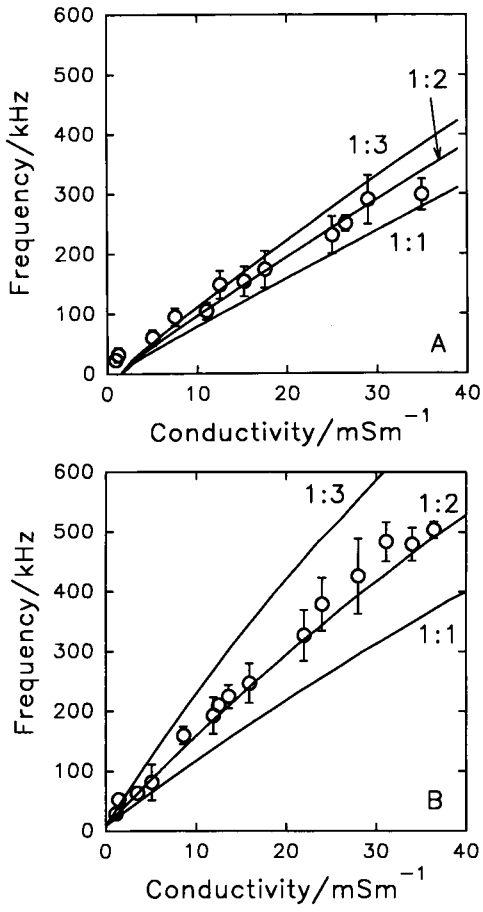

FIGURE 4 (*A*) Dependence of the first critical frequency of dielectrophoresis; and (*B*) The first characteristic frequency of electrorotation of control cells on the external conductivity. Every point represents frequency values of 7 to 15 cells. Curves represent three different axis ratios for the ellipsoidal model indicated in the figures.

At higher ionophore concentrations, measurements were only possible for a shorter period of time unless a decrease in the rotation was too pronounced to allow exact compensation method measurements. The average of data belonging to the first characteristic frequency (Fig. 5) and the rotation (Fig. 6) were plotted. For these figures time classes of 1-min width were established. For every time class about 10 values were obtained. For a more comprehensive representation the deviations, which mainly reflected differences of individual cells, are not shown. First characteristic frequency and rotation peak deviated less than ±30kHz and ±0.05 × 10^{-7} $radm^2/sV^2$, respectively.

Check for a transient increase of the first characteristic frequency after ionophore application

Usually the first characteristic frequency could only be measured one and a half minutes after introducing the cells into the ionophore solution. To check whether a transient increase of the first characteristic frequency exists, the chamber was filled with ionophore free cell suspension. The compensation

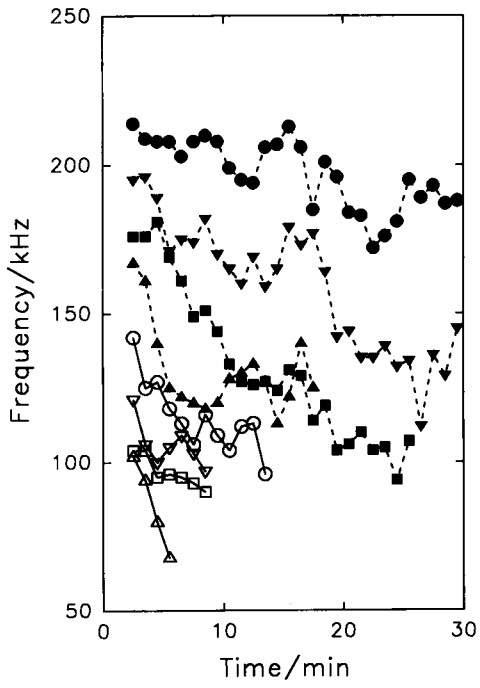

FIGURE 5 Dependence of the first characteristic frequency on time under the influence of different ionophore concentrations. Curves with steeper slopes represent higher nystatin concentrations. Concentrations of 0 (●), 10 (▼), 15 (■), 20 (▲), 25 (○), 30 (▽), 35 (□), and 40 (△) μg/ml were used.

field was adjusted to a frequency at which the rotation of the cells ceased. Then the same volume of cell free ionophore solution was added. According to the compensation principle, a change of the first characteristic frequency would reestablish the rotation. The sense of that rotation would depend on whether the first characteristic frequency increases or decreases. Even this fast procedure could not detect an increase of the first characteristic frequency.

DISCUSSION

Ionic states of erythrocytes

When the suspension medium of erythrocytes is changed these cells undergo a sequence of transiently stable cell states. By far the fastest process is the osmotic equilibration, which is followed by an equilibration of pH, Cl^-, and other anions. The cells reach the so called C-state. For this transiently stable ionic state ion content and cell volume can be calculated assuming the corresponding equilibrium conditions (Glaser, 1982; Glaser and Donath, 1984). Although for calculations an isotonic measuring solution was assumed, the cytoplasmic Cl^--concentration in the C-state is decreased. This is the result of the low ionic strength in the external solution. Thus the cells are shrunken (Glaser, 1982). After equilibration of the cations Na^+ and K^+ the cells reach the Donnan osmotic equilibrium (D-state). This process is accompanied by further shrinkage and can be enhanced by ionophores. Unfortunately, within the first minutes after suspension into the measuring solution, no simple assumptions for the calculation of the cells' ionic state are possible.

Calculated cytoplasmatic ion concentration and measured internal conductivity

To calculate the cell ionic content and volume of the C- and D-states the following conditions were taken for the physiological state (100% cell-volume) (Glaser and Donath, 1984): The cell water occupies 71% of the cell volume. Temperature, pH, hemoglobin concentration, Na^+- plus K^+-ionic concentration in cell water, and the summarized external osmotic pressure were assumed to be 23°C, 7, 7 mM, 146 mM, and 300 mOsm, respectively. Thus, at 100% cell volume the sum of internal-concentration of monovalent cat- and anions, which contribute to the cytoplasmic conductivity, is about 207 mM for the cell volume. For calculation of the C-state an external Cl^--concentration of 1 mM and no cation-exchange was assumed. C- and D-ionic state were calculated numerically using an iterative method (Glaser, 1982; Glaser and Donath, 1984). The C-state is characterized by a decreased Cl^--concentration. Because of this loss of osmotically active ions the cell volume is decreased as well. For the calculation of the D-state (Donnan-equilibrium), K^+- and Na^+-ions were assumed to be in electrochemical equilibrium. Results are presented in Table 2.

The ions not considered in the model, such as Mg^{2+}, HCO_3^-, as well as hemoglobin, yield only a small contribution to the cytoplasmic conductivity. Thus, it is justified to estimate the cytoplasmatic conductivity from the sum of monovalent ions. Under assumption of an ideal electrolyte solution, calculation of the internal conductivity for the physiological cell-state from the ion concentration given in

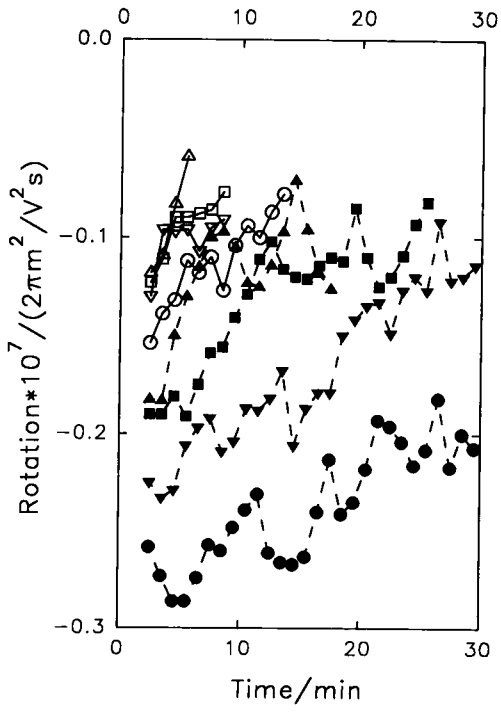

FIGURE 6 Dependence of the antifield rotation peak on time under the influence of different ionophore concentrations. Concentrations used are indicated in Fig. 5.

TABLE 2 Calculated cytoplasmic ion concentrations per cell volume of erythrocytes suspended in isotonic solution of 1 mM NaCl, pH 7

	Relative Cell Volume (%)	Cl^- (mM)	$Na^+ + K^+$ (mM)	Sum of Monovalent Ions (mM)
Physiological cell-state	100	103.6	103.6	207.3
C-state	73	26.0	142.6	168.6
D-state	48	0.7	0.5	1.2

Table 1 yields about 1.1 S/m. This value is much higher than experimentally found (Fig. 1). The reason for this is a reduced ion mobility as the result of the high hemoglobin concentration (Pauly and Schwan, 1966).

For the C-state the volume decrease is hampered by the relative increase of the nonpermeable molecule concentration (see Appendix). Thus, the decreased ion concentration is only partly compensated by shrinkage, and the cytoplasmic conductivity is decreased.

For the D-state there is obviously a discrepancy between measured conductivities and the model internal ion concentration. In the case of D-state, cell handling was not as easy as for native and C-state cells. Values for hematocrits close to 100% could not be determined. The fitted curve is much flatter, and thus the extrapolated value for the 100% hematocrit is not as reliable. Impurities caused by displaced ions entrapped by the glycocalix would have a much more pronounced effect than in the other two cases. In addition, calculated internal ion concentrations for the D-state are more sensitive to the model parameters, e.g. pH, than in the case of the C-state.

Volume dependence

To consider the time dependence of the volume, a simple model was applied (Appendix). It was assumed that cells under physiological conditions possess a cell volume (V_0) of 98 μm^3 and a cell surface area (A) of 133 μm^2 (Engström et al., 1992; Jay and Canham, 1977). For nonlinear regression, points of increasing volumes after the initial drop were not considered.

From the nonlinear regression for all curves, a starting volume (V_0) of 88.3% was found. Calculated membrane permeabilities are given in Fig. 2. The theoretical cell volume calculated from the ionic state model given in Table 2 for the C-state corresponds to the volume of control cells after 30 min of incubation in the measuring solution. The predicted volume for the Donnan osmotic equilibrium of 48% is in good agreement with the fitted minimal volume (V_e) of 50 μm^3 corresponding to 51% of the physiological volume. The latter volume is reached at a nystatin concentration of 40 $\mu g/ml$ after 6 min. Georgiewa et al. (1989*b*) used the micropipette aspiration technique to check the dependence of the erythrocyte volume on the osmotic pressure in a 1-mM phosphate buffer sucrose solution. Their procedure took about 20 min. For 300 mOsm they found volumes in between the theoretically predicted C- and D-state volumes. This is in accordance to our control cell curve (Fig. 7).

Dielectric parameters of control cells

The simplest way to qualitatively describe the dielectric behavior of erythrocytes is to invoke the spherical single-shell model. It has been applied in connection with different methods for dielectric spectroscopy, e.g., impedance measurements (Bao et al., 1992; Fricke, 1953; Pauly and Schwan, 1966), dielectrophoresis (Burt et al., 1990; Gascoyne et al., 1993), and electrorotation (Engel et al., 1988; Gimsa et al., 1988, 1989).

Although dielectrophoresis and electrorotation are strongly interrelated (Gimsa et al., 1991; Huang et al., 1992; Kaler and Jones, 1990; Wang et al., 1992) for various cell species, different parameters for internal and membrane conductivity, as well as for membrane capacitance were found. Discrepancies were contributed to additional relaxation processes caused by internal membrane systems (Fuhr et al., 1985; Gimsa et al., 1991). In the case of erythrocytes no such systems exist. In addition, all electrorotation spectra measured, suggest only one relaxation process in the frequency range of membrane dispersion (see Fig. 3). Because of the high measuring frequencies the influence of the surface conductivity on the spectra can be neglected (Burt et al., 1990; Gascoyne et al., 1993). The effective complex cell permittivity strongly depends on the cell geometry. Therefore, it can

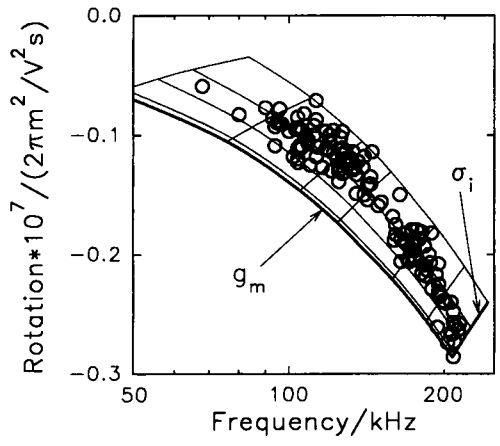

FIGURE 7 Measuring points represent the antifield rotation peak and corresponding first characteristic frequencies (see f_{c1} and R_{min} in Fig. 3) for all ionophore concentrations applied. The network diagram represents theoretical frequency and peak height of the antifield rotation peak, calculated for control cell parameters. The network diagram was obtained by variation of internal- and membrane- conductivity. For calculations we assumed the long half axis, axis ratio, internal dielectric constant, membrane capacitance, external dielectric constant, and the external conductivity to be 3.3 μm, 1:2, 50, 0.82 $\times$ 10^{-2} F/m^2, 80, and 12.5 mS/m, respectively. To fit the network to the control cell data the theoretical peak heights were normalized. Lines of constant membrane conductivity, g_m, represent 0 (*bold line*), 100, 500, 1000, and 2000 S/m^2. Lines of constant internal conductivity, σ_i, represent 600 (*bold line*), 200, 100, 50, 35, 20, and 10 S/m.

be understood that the fit of experimental data of nonspherical cells to the spherical model yield inconsistent values for the dielectric cell properties. To address the discrepancy of the membrane capacitances found from dielectrophoresis and electrorotation, we varied the ratios of the axes of an oblate, confocal single-shelled ellipsoidal model of rotational symmetry (for mathematical details see Müller et al., 1993). To our knowledge it is the first time that, besides the nonspherical cell geometry, the transmembrane conductivity has been taken into account to describe the interaction of erythrocytes with electric fields.

In electrorotation the flat biconcave erythrocytes rotate with their axis of symmetry perpendicular to the plane of field rotation. In dielectrophoresis, they move with the axis of symmetry perpendicular to a line, connecting tip and plane electrode. Although the ellipsoidal model does not accurately model the erythrocyte shape, we established a certain axis ratio that allows a sufficiently good description for the frequency range below 1 MHz in the following way: the first critical frequency and the first characteristic frequency were measured over an external conductivity range of 0.1–40 mS/m (Fig. 4, *A* and *B*). The two frequency curves of our model were fitted to the data by variation of axis ratio and dielectrical parameters of the membrane. The internal conductivity, the long half-axis, and the internal dielectric constant were fixed at 0.535 S/m (see Table 1), 3.3 μm (microscopic measurements), and 50 (see Pauly and Schwan, 1966), respectively. By extrapolating the first characteristic frequency curve to the frequency axis, a membrane conductivity of 480 S/m^2 was found. We found that for the ellipsoidal model, this point and the conductivity where negative dielectrophoresis disappears (see Fig. 4, *A* and *B*) are almost independent of the axis ratio. The latter influences the slopes of the frequency curves over external conductivity, mainly that of the first characteristic frequencies. From these considerations an axis ratio of 1:2 and a membrane capacitance of 0.82×10^{-2} F/m^2 were found. Interestingly, dielectrophoresis measurements suggest a much lower membrane conductivity than electrorotation. In our opinion this can be related to the qualitatively different field distribution at the membrane for the two methods. For electrorotation the whole equatorial plane, which is identical to the plane of the rotating field, is exposed to a constantly high field strength. If this field strength is that necessary to drive ions through the membrane by a process as proposed by electroconformational coupling models, one can expect to measure a high membrane conductivity. This is not the case for dielectrophoresis. For the same field strength only a much smaller membrane area would be exposed to the necessary field strength. The membrane spot facing the tip electrode experiences a much higher field stress. This possibly drives transport into saturation, whereas most of the membrane experiences a field strength that might not be able to overcome the activation energy necessary for ions to cross the membrane (Markin et al., 1992).

Ionophore influence on dielectric data

Ionophore treatment changes the cell shape in a complex way. Two general factors must be considered. Shrinkage diminishes the overall cell radius. On the other hand, the specific shape transformation during shrinkage increases the radius of curvature at the cell equator, the site where the highest contribution to the induced dipole moment is located. With respect to the relaxation time of the membrane, these two contributions counteract. Unless erythrocytes do not show membrane surface area changes during shape transitions, the overall membrane capacitance remains constant. For these reasons, and to simplify calculations, we assumed a constant membrane capacitance and cell geometry during experiments. Besides changes in the geometry, the ionophore-induced increase of membrane permeability causes ions to be transported across the membrane, which increases the number of charge carriers in the membrane and, in turn, should increase the membrane conductivity. On the other hand, an increase in membrane permeability leads to ion leakage and a subsequent decrease of the intracellular ion concentration. The assumption of a permeability increase for cations induced by ionophore action at the time of cell suspension leads to a decrease of internal conductivity down to a value on the order of the very low external conductivity. Ion leakage such as this can only cause a decrease of the first characteristic frequency. For a better understanding of ionophore-induced changes of dielectric parameters, a network diagram depicting antifield rotation and the first characteristic frequency (see Fig. 3) in dependence on the model parameters was developed (Fig. 7). Except for varied membrane and internal conductivities, parameters of control cells were used for the calculation of the network response characteristics.

To fit theoretical electrorotation peak heights to measured data, the former were normalized to correct for hydrodynamic friction. Despite strong deviations a definite trend can be established; the membrane conductivity for the first points of control cells, with high internal conductivities, scatter around the value of 480 S/m^2, ranging from 0–1000 S/m^2. Independently of nystatin concentration, the decrease of internal conductivity performs at a constant or even increasing membrane conductivity.

Internal properties

The data points of Fig. 7 were transformed to obtain the dependence of internal conductivity on time.

The time course was interpreted phenomenologically for control cells and nystatin concentrations up to 25 μg/ml by fitting a simple single exponential function:

$$\sigma_i = a + be^{-\pi}. \quad (4)$$

Too few data points were measured, for higher ionophore concentrations. From τ, permeabilities can be estimated assuming native cell volume and membrane surface area. For control cells, at the time of first electrorotation measurements (2.5 min), a good agreement with internal conductivity of the

control of hemolysis experiments (Fig. 1) can be seen. Interestingly, conductivity falls far below the value of 460 mS/m expected from hemolysis after 30 min (Fig. 1) and from the number of internal ions found from calculations of the C-state (Table 1). This contradiction can only be explained by assuming that there is a strong increase of the hindrance for ion movement because of cell shrinkage and a subsequent hemoglobin concentration increase. Electron spin resonance-correlation-time measurements detecting the microviscosity experienced by a label molecule support this view (Herrmann and Müller, 1986). For erythrocytes in low ionic strength solution these authors found a strongly increasing hindrance for the rotation of the spin-label molecule Tempone. Because the effective radii of this label and hydrated ions are of the same order, a similar decrease of mobility must be expected. For hemoglobin solutions and the inside of shrunken cells, an exponential increase of microviscosity with increasing hemoglobin concentration was found. The microviscosity detected by electron spin resonance increased by a factor of 1.8 and 3.4 when erythrocytes shrunk from 100% of their physiological volume to 68 and 50%, respectively. Comparison of the cytoplasmic conductivity obtained from hemolysis (Fig. 1, *inverted triangles*) with that from Fig. 8 (Table 3) after 30 min of suspension (cells in C-state at 68% of their physiological volume) suggests a higher hindrance factor for ions. In contrast to Tempone, it must be assumed for ions that their number, which is tightly associated with hemoglobin, increases. On the other hand, shrinkage decreases the amount of cell water, and, similarly, the percentage of water in the hydration zone of hemoglobin increases. This hydration water is believed not to dissolve ions (Pauly and Schwan, 1966). Cytoplasmic conductivity values, obtained from electrorotation of control cells immediately after suspension, are consistent with the results of hemolysis (Fig. 1). They suggest a hindrance factor of 2, which was already found by Pauly and Schwan (1966). Unless the internal conductivity falls below the expected value of 460 mS/m by a factor of about 3 at 68% cell volume, an overall hindrance of about 6 must be assumed. In the case of nystatin-treated cells at Donnan equilibrium, a conductivity value of about 5 mS/m, being less than the external conductivity, was calculated. For this case model calculations and hemolysis experiments do not agree. One reason for a higher value obtained from hemolysis might be that conductivity of hemoglobin and associated ions was not taken into account. We expected a pH dependence of this conductivity as a result of a pH-depending ion association and the charge number of hemoglobin. By titration of hemolyzed cells within the pH-range of 5.6–7.4 we found that the conductivity is almost independent of medium pH. For nystatin-treated cells with volumes below 68% a hindrance factor higher than 6 must be expected. This range of hemoglobin concentration, giving rise to an extremely nonlinear hindrance increase, cannot be reached by hemolysis experiments.

TABLE 3 Recalculated internal conductivities for ionophore concentrations

Ionophore Concentration (μg/ml)	Permeability (m/s)	Extrapolated Internal Conductivity (mS/m)
0	6.5×10^{-10}	605
10	8.3×10^{-10}	192
15	1.2×10^{-10}	125
20	1.1×10^{-9}	81
25	1.1×10^{-9}	57

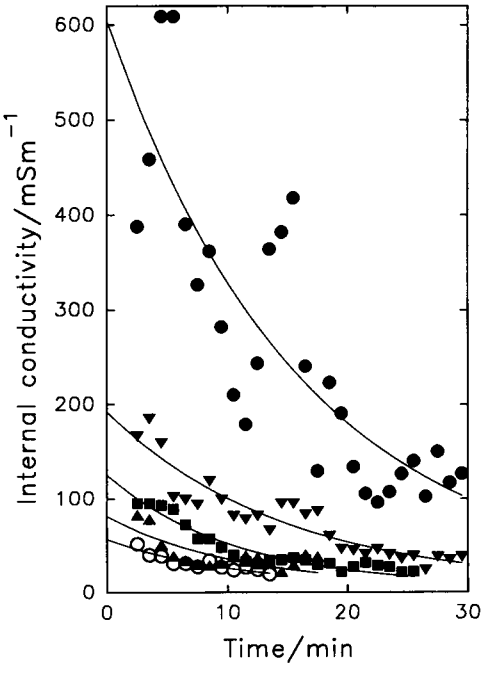

FIGURE 8 Recalculated internal conductivities for ionophore concentrations of 0 (control, ●), 10 (▼), 15 (■), 20 (△), and 25 μg/ml (○) are plotted. The membrane permeabilities were estimated from the fit of Eq. 4. To obtain internal conductivity values, curves were extrapolated to time 0 min.

For all ionophore data, the time course of internal conductivity could only be fitted by a single exponential when starting values, decreasing with increasing ionophore concentrations, were used (Fig. 8). This behavior suggests, that rapid shrinkage after cell transfer contributes to the reduction of internal conductivity even more than the loss of ions. This concept is consistent with permeabilities estimated from Fig. 8. A comparison with the permeabilities found from Coultercounter measurements (Fig. 2) gives very similiar values for higher nystatin concentrations. This proves that in these cases the same mechanism, namely the loss of ions, is responsible for the drop of internal conductivity. This is also true for the concentrations higher than 25 μg/ml that were not plotted. For control, a discrepancy of a factor of 3 decreasing to about 1.4 at an ionophore concentration of 15 μg/ml is found. In these cases, both factors, ion loss and the reduction of effective ion mobility, are responsible for the internal conductivity decrease.

Membrane properties

Our data (Figs. 4 *B* and 7) show a high membrane conductivity for erythrocytes in the frequency range from 20–200kHz. This conductivity can be attributed to the high exchange permeability caused by band 3 protein (Donath et al, 1990; Engel et al., 1988). From simple electrochemical considerations membrane conductivity can be shown to be proportional to membrane permeability and effective membrane ion concentrations (Engel et al., 1988; Gimsa et al., 1989). Membrane conductivity, in general, cannot be independent of the intracellular ion concentration. If the intracellular ion concentration changes, ion partition or ion binding to membrane protein binding sites will also change. A lower internal ion concentration should decrease the number of charge carriers able to cross the membrane, which should cause a decrease of the membrane conductivity. Considerations reveal that nystatin permeability necessary to induce a membrane conductivity contribution on the order of magnitude of the control, would cause an instantaneous loss of cytoplasmic ions. So, at most, only a transient membrane conductivity increase can be expected. If this increase is large enough, it should cause a transient increase of the first characteristic frequency. This could not be found experimentally.

CONCLUSION

The ellipsoidal model can solve discrepancies of membrane capacitances and cytoplasmic conductivities found by dielectrophoresis and electrorotation in the frequency range of membrane relaxation. Unless dielectrophoresis and electrorotation experiments can be conducted only at low ionic strength, one should be aware that, even for control cells, a rapid dielectric property change because of changes of the cells' ionic state occurs. Thus, experiments should be carried out within less than 5 min. The main reason for the internal conductivity drop of control cells is the increase of hindrance caused by cell shrinkage. The discrepancy of different membrane conductivities found for control cells from dielectrophoresis and electrorotation persists. In the case where the high electrorotation value reflects the actual membrane-AC conductivity, the existing model (Donath et al., 1990) needs some reconsideration, because a decrease of membrane conductivity with decreasing internal ion concentration could not be found.

APPENDIX

Osmotic Model of Volume Changes

For measurements cells were suspended at a hematocrit of 0.02%. Thus the external osmotic pressure was assumed not to change because of ionic leakage from the cells. Larger molecules like hemoglobin, ADP, hexoses, etc. were assumed not to penetrate the membrane. Internal osmotic pressure is given by the sum of the number of penetrable ions (n_{Ion}) and nonpenetrable molecules (n_{Mol}). Both species are assumed to be homogeneously distributed inside the cell. At any time the internal osmotic pressure is equal to the external

$$\frac{n_{Ion}}{V} + \frac{n_{Mol}}{V} = \text{const.} \tag{A1}$$

In Eq. A1 n_{Ion} and the cell volume V are functions of time. Differentiation leads to

$$\frac{dn_{Ion}}{dt} = \frac{n_{Ion} + n_{Mol}}{V}\frac{dV}{dt}. \tag{A2}$$

At any time the decrease of n_{Ion} is limited by the loss of a certain ionic species because the loss of counter ions is restricted by the condition that the cell interior has to stay electroneutral. Using these assumptions the specific membrane permeability, P, of the limiting ionic species can be introduced by

$$\frac{dn_{Ion}}{dt} = -\frac{PAn_{Ion}}{V} \tag{A3}$$

where A is the cell surface area. Introduction of Eq. A3 into Eq. A2 rearrangement of the terms and integration within the boundaries from 0 to t and V_0 to V, respectively, leads to

$$t = \frac{V_0 - V}{PA} - \frac{V_e}{PA}\log\frac{V - V_e}{V_0 - V_e}. \tag{A4}$$

where the final volume V_e was assumed to be

$$V_e = \frac{n_{Mol}}{n_{Ion} + n_{Mol}} V. \tag{A5}$$

We are grateful to P.I. Kuzmin for helpful discussions. S. Diez and M. Brown are acknowledged for help with the manuscript.

This study was supported by grant #I/66158 from Volkswagen-Stiftung.

REFERENCES

Arnold, W. M., and U. Zimmermann. 1983. Patent application, P3325843.0, Germany.

Asami, K., T. Hanai, and N. Koizumi. 1980. Dielectric approach to suspensions of ellipsoidal particles covered with a shell in particular reference to biological cells. *Jap. J. Appl. Phys.* 19:359–365.

Asami, K., Y. Takahashi, and S. Takashima. 1989. Dielectric properties of mouse lymphocytes and erythrocytes. *Biochim. Biophys. Acta.* 1010: 49–55.

Bao, J. Z., C. C. Davis, and R. E. Schmukler. 1992. Frequency domain impedance measurements of erythrocytes. *Biophys. J.* 61:1427–1434

Burt, J. P. H., R. Pethig, P. R. C. Gascoyne, and F. F. Becker. 1990. Dielectrophoretic characterisation of Friend murine erythroleukaemic cells as a measure of induced differentiation. *Biochim. Biophys. Acta.* 1034: 93–101

Donath, E., V. Ph. Pastushenko, and M. Egger. 1990. Dielectric behavior of the anion-exchange protein of human red blood cells. *Bioelectrochem. Bioenerg.* 23:337–360.

Engel, J., E. Donath, and J. Gimsa. 1988. Electrorotation of red cells after electroporation. *Stud. Biophys.* 125:53–62.

Engström, K. G., B. Möller, and H. J. Meiselman. 1992. Optical Evaluation of red blood cell geometry using micropipette aspiration. *Blood Cells.* 8:241–258.

Fricke, H. 1953. Relation of the permittivity of biological cell suspensions to fractional cell volume. *Nature (Lond.).* 172:731–732.

Fuhr, G., J. Gimsa, and R. Glaser. 1985. Interpretation of electrorotation of protoplasts. *Stud. Biophys.* 108:149–164.

Fuhr, G., R. Glaser, and R. Hagedorn. 1986. Rotation of dielectrics in a rotating high frequency field; model experiments and theoretical explanation of the rotation effect of living cells. *Biophys. J.* 49:395–402.

Gascoyne, P. R. C., R. Pethig, J. P. H. Burt, and F. F. Becker. 1993. Membrane changes accompanying the induced differentiation of Friend murine erythroleukaemic cells studied by dielectrophoresis. *Biochim. Biophys. Acta.* 1149:119–126.

Georgiewa, R., E. Donath, J. Gimsa, U. Löwe, and R. Glaser. 1989*a*. AC-field-induced KCl leakage from human red cells at low ionic strength. *Bioelectrochem. Bioenerg.* 22:255–270.

Georgiewa, R., E. Donath, and R. Glaser. 1989*b*. On the determination of human erythrocyte intracellular conductivity by means of electrorotation —influence of osmotic pressure. *Stud. Biophys.* 133:185–197.

Gimsa, J., E. Donath, and R. Glaser. 1988. Evaluation of data of simple cells by electrorotation using square-topped fields. *Bioelectrochem. Bioenerg.* 19:389–396.

Gimsa, J., P. Marszalek, U. Löwe, and T. Y. Tsong. 1991. Dielectrophoresis and electrorotation of neurospora slime and murine myeloma cells. *Biophys. J.* 60:5–14

Gimsa, J., C. Pritzen, and E. Donath. 1989. Characterization of virus-red-cell interaction by electrorotation. *Stud. Biophys.* 130:123–131.

Glaser, R. 1982. Echinocyte formation by potential changes of human red blood cells. *J. Membr. Biol.* 66:79–85.

Glaser, R., and J. Donath. 1984. Stationary ionic states in human red blood cells. *Bioelectrochem. Bioenerg.* 13:71–84.

Herrmann, A., and P. Müller. 1986. Correlation of the internal microviscosity of human erythrocytes to the cell volume and the viscosity of hemoglobin solutions. *Biochim. Biophys. Acta.* 885:80–87.

Huang, Y., R. Hölzel, R. Pethig, and X.-B. Wang. 1992. Differences in the AC electrodynamics of viable and non-viable yeast cells determined through combined dielectrophoresis and electrorotation studies. *Phys. Med. Biol.* 37:1499–1517.

Irimajiri, A., T. Suzaki, K. Asami, and T. Hanai. 1991. Dielectric modeling of biological cells. Models and algorithm. *Bull. Inst. Chem. Res. Kyoto Univ.* 69:421–438.

Jay, A. W. L., and P. B. Canham. 1977. Viscoelastic pro- perties of the human red blood cell membrane. II. Area and volume of individual red cells entering a micropipette. *Biophys. J.* 17:169–178.

Kaler, K. V. I. S., and T. B. Jones. 1990. Dielectrophoretic spectra of single cells determined by feedback-controlled levitation. *Biophys. J.* 57: 173–182.

Kaler, K. V. I. S., J.-P. Xie, T. B. Jones, and R. Paul. 1992. Dual-frequency dielectrophoretic levitation of Canola protoplasts. *Biophys. J.* 63:58–69.

Kinosita, Jr., K., and T. Y. Tsong. 1977. Voltage-induced pore formation and hemolysis of human erythrocytes. *Biochim. Biophys. Acta.* 471: 227–242.

Markin, V. S., D.-S. Liu, J. Gimsa, R. Strobel, and M. D. Rosenberg. 1992. Ion channel enzyme in an oscillating electric field. *J. Membr. Biol.* 126: 137–145.

Marszalek, P., J. J. Zielinsky, M. Fikus, and T. Y. Tsong. 1991. Determination of electric parameters of cell membranes by a dielectrophoresis method. *Biophys. J.* 59:982–987.

Miller, R. D., and T. B. Jones. 1993. Electro-orientation of ellipsoidal erythrocytes. *Biophys. J.* 64:1588–1595

Müller, T., L. Küchler, G. Fuhr, T. Schnelle, and A. Sokirko. 1993. Dielektrische Einzelzellspektroskopie an Pollen verschiedener Waldbaumarten-Charakterisierung der Pollenvitalität. *Silvae Genet.* 42:6:311–322.

Pastushenko, V. Ph., P. I. Kuzmin, Yu. A. Chizmadshev. 1985. Dielectrophoresis and electrorotation: a unified theory of spherically symmetrical cells. *Stud. Biophys.* 110:51–57.

Paul, R., and M. Otwinowski. 1991. The theory of the frequency response of ellipsoidal biological cells in rotating electrical fields. *J. Theor. Biol.* 148:495–519.

Pauly H., and H. P. Schwan. 1966. Dielectric properties and ion mobility in erythrocytes. *Biophys. J.* 6:621–639.

Stenger D. A., K. V. I. S. Kaler, and S. W. Hui. 1991. Dipole interactions in electrofusion. *Biophys. J.* 59:1074–1084.

Stepin, L. D. 1965. Dielectric permeability of a medium with non-uniform ellipsoidal inclusions. *Sov. Phys.- Tech. Phys.* 10:768–772.

Wang, X.-B., R. Pethig, and T. B. Jones. 1992. Relationship of dielectrophoretic and electrorotation behaviour exhibited by polarized particles. *J. Phys. D Appl. Phys.* 25:905–912.